

SiO₂-Based Nanofluids for the Inhibition of Wax Precipitation in Production Pipelines

Daniel López, As A. Ríos, Juan D. Marín, Richard D. Zabala, Jaime A. Rincon, Sergio H. Lopera, Camilo A. Franco,* and Farid B. Cortés*



Cite This: *ACS Omega* 2023, 8, 33289–33298



Read Online

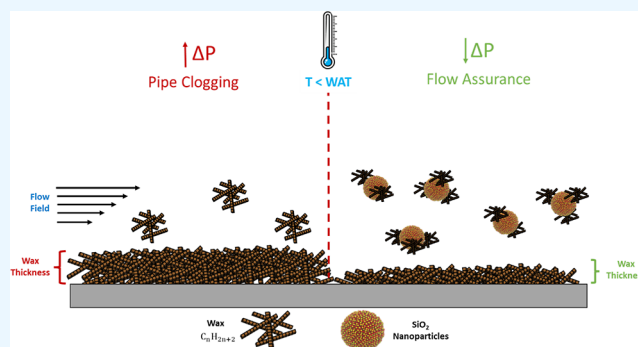
ACCESS |

Metrics & More

Article Recommendations

Supporting Information

ABSTRACT: Wax deposition in high-wax (waxy) crude oil has been an important challenge in the oil and gas industry due to the repercussions in flow assurance during oil extraction and transportation. However, the nanotechnology has emerged as a potential solution for the optimization of conventional wax removal and/or inhibition processes due to its exceptional performance in the alteration of wax morphology and co-crystallization behavior. In this sense, this study aims to study the performance of two commercial wax inhibitor treatments (WT1 and WT2) on the wax formation and crystallization due to the addition of SiO₂ nanoparticles. Differential scanning calorimetry experiments and cold finger tests were carried out to study the effect of the WT on wax appearance temperature (WAT) and the wax inhibition efficiency (WIE) in a scenario with an initial temperature difference. In the first stage, the behavior of both WT in the inhibition of wax deposition was achieved, ranging in the concentration of the WT in the waxy crude (WC) oil from 5000 to 50,000 mg·L⁻¹. Then, NanoWT was prepared by the addition of SiO₂ nanoparticles on WT1 and WT2 for concentrations between 1000 and 500 mg·L⁻¹, and the performance of the prepared NanoWT was studied at the best concentration of WIT in the absence of nanoparticles. Finally, the role of the nanofluid concentration in wax inhibition was accomplished for the best NanoWT. Selected NanoWT with nanoparticle dosage of 100 mg·L⁻¹ added to WC oil at 5000 mg·L⁻¹ displays reductions in WAT and WIE of 15.3 and 71.6 for NanoWT1 and -2.2 and 42.5% for NanoWT2. In flow loop experiments for the crude oil at temperatures above (30 °C) and below (16 °C), the WAT value indicates an increase of 8.3 times the pressure drops when the crude oil is flowing at a temperature below the WAT value. Therefore, when NanoWT1 is added to the crude oil, a reduction of 31.8% was found in the pressure drop in comparison with the scenario below the WAT value, ensuring the flow assurance in the pipeline in an unfavorable environment. Based on the pressure-drop method, a reduction greater than 5% in the wax deposit thickness confirms the wax deposition inhibitory character of the designed NanoWT.



1. INTRODUCTION

Nowadays, fossil fuels represented in crude oil, coal, and natural gas are the most prominent energy sources in the post-pandemic reactivation accounting for 1000 TWh in electricity generation and will provide nearly 80% of the global energy demand in the next decade.¹ This scenario pushes the energy sector to innovate and exploit non-conventional oil such as waxy crude (WC) oil with more than 20% of the global oil reserves.^{2–4} According to Philp et al.,⁵ wax compounds correspond to normal and branched long-chain alkenes with relatively low carbon numbers (C₂₀ to C₅₀). Generally, wax molecules are dissolved in a balanced state in crude oil under reservoir conditions,^{6–10} however, when the temperature of the crude oil falls below the wax appearance temperature (WAT) since WAT is approximating the thermodynamic solubility limit of the wax. Below this temperature, wax molecules tend to precipitate from crude oil matrix, forming

wax crystals, and getting deposited onto pipe surfaces.^{11–13} In this respect, wax precipitation produces deposits on pipe walls and progressively clogs the production causing restriction in the flow, abnormal pressure drops, fluid gelation, lower flowability, and higher pumping costs.^{14–17} In addition to temperature, other factors that affect the wax solubility and precipitation degree are related to the crude oil composition,^{15,18} the gas–oil ratio,^{19–21} the water–oil ratio,^{22–25} pressure,¹⁵ flow rate,¹⁵ and inner pipe-surface roughness.^{15,26,27}

Received: March 27, 2023

Accepted: July 21, 2023

Published: September 8, 2023



as well as the presence of asphaltene aggregates, which are known to provide sites for wax crystal buildup.²⁸

Wax crystallization can be resumed in three stages, corresponding to (i) nucleation, (ii) growth, and (iii) agglomeration.^{29,30} In the first stage, the first nuclei start to appear when the solution temperature is lower than WAT, limiting the wax thermodynamic solubility of the wax and inducing the formation of wax crystals.³¹ Then, the wax crystal size increases adopting morphologies such as plates, and needles, among others.³² Once the first crystals appear, they begin to grow by binding wax crystals due to attractive intermolecular forces such as van der Waals forces.³³ Hence, during the agglomeration stage, a three-dimensional wax structure is produced, and a solid-like gel is formed.³⁰ Three-dimensional wax can change the flowing behavior of the crude oil from Newtonian to non-Newtonian (pseudoplastic at temperatures near the pour point and Bingham at temperatures below the pour point) and may lead to higher effective viscosities.

Several methods have been proposed to prevent and remediate wax deposition,^{34–40} nonetheless, conventional methods are usually expensive and may lead to the formation damage and stuck-up instruments inside the tubing.³⁴ In recent years, chemical inhibition methods have received a lot of attention due to their high impacts on production and improvement of the flow properties of paraffinic crude oil,^{25,41–43} however, the efficiency of chemical inhibitors can be affected depending on the type of crude oil and the specific chemical composition.⁴² A chemical wax inhibitor can be divided into three main groups: wax dispersants, pour point depressants (PPDs), and wax crystal modifiers.²⁵ Wax dispersants are associated with surfactant compounds which tend to get adsorbed onto the pipe wall surface, decreasing the wax adhesion due to the alteration of the wall wettability or by the formation of thin layers that induce the wax crystals shear off easily.^{25,44} Besides, a wax dispersant can adsorb on the wax crystals creating a wax crystal lattice that alters the morphology of the growing wax crystals. Commonly, wax crystallization tends to form a “house-of-card” type structure, where the wax crystals overlap and interlock within them, forming a three-dimensional network. Wax dispersants provide different sites for the wax nucleation, affecting the growth and shape of the wax crystals. In this sense, the wax crystallization process is hindered due to the formation of plate-like or lamellar structures, so the modified wax crystals cannot interlock each other, and the formation of three-dimensional structures is delayed.^{25,41,45,46}

Wax dispersants are expected to increase the crude oil flow properties, reducing the pour point due to their capacity to alter the morphology as well as reducing wax co-crystallization.⁴⁷ Otherwise, PPDs are mostly polymers that co-crystallize into the wax structure via van der Waals forces inducing a steric/entropic repulsion among the wax crystals.^{25,48} PPDs do not inhibit the wax crystallization (i.e., decrease in the WAT) but instead inhibit the growth of the wax crystals, affecting the crude oil pour point temperature.⁴⁹ The use of PPDs allows the easy removal of the deposition by shear forces due to its capacity to weaken the wax deposition solid structure.^{25,42,49,50} Finally, the incorporation of wax crystal modifier during the nucleation process changes the growth and surface characteristics of the wax crystals causing the formation of micelle-like aggregates.^{51,52} Therefore, a subcritical nucleus is formed reducing the supersaturation

properties of the crude oil (i.e., decreasing the wax appearance point). Besides, wax crystal modifiers can diminish the tendency to form a three-dimensional structure, which reduce the pour point and the oil viscosity.^{25,52}

Nanotechnology is a rapidly growing field that may supply an alternative to the currently available techniques for paraffin wax inhibition.^{44,52–56} Due to their high stability, high adsorptive capability, and excellent dispersion ability, nanoparticles can lower the number of wax deposits formed, reduce the crystallization temperature, and diminish the possibilities of wax aggregation.^{52,57} Previous studies have confirmed the ability of nanoparticles to inhibit paraffin wax deposition. According to Ridzuan et al.,⁵³ the nanoparticles aid in better dispersion of wax crystals promoting the formation of low-size aggregates, affecting the wax-particle interactions, and thus reducing the deposition of wax onto surfaces. In this sense, Vakili et al.⁴⁴ suggest that the nanoparticle mechanism in the inhibition of wax deposition is strongly dependent on the nanomaterial to wax aggregates size ratio. In this respect, when the nanoparticles are larger than the wax nuclei, the wax tends to be physically adsorbed onto the nanoparticle surface, so the nucleation is altered from homogeneous nucleation to heterogeneous nucleation, and the wax crystal growth is slowed down. When the nanoparticles are smaller than the wax crystal, the nanomaterials tend to surround the crystal nuclei serving as a steric hindrance agent, and thus preventing the aggregation of the nearby crystal nuclei. In this scenario, the nanoparticles reduce the wax-particle clustering and promote a more homogeneous wax crystal size distribution. Finally, if the nanoparticle size is close to the wax nuclei size, the nanomaterials promote the formation of low-size wax crystals acting as nucleation centers and inhibiting the clustering among them.

Song et al.⁵⁴ demonstrated that the presence of asphaltenes and resins directly affects the number of formed wax crystals, WAT, PP, and rheological parameters of model oils when a nanofluid, formed by xylene with 1 wt % of SiO₂ nanoparticles, was added. Due to their high adsorption affinity and large surface area-to-volume ratio, asphaltenes and resins were adsorbed on the surface of SiO₂ nanoparticles, preventing their aggregation. As result, nanoparticles impeded the nucleation of wax crystals on asphaltene aggregates, and hence, the crystallization temperature was reduced. Lim et al.⁵⁵ investigated the wax deposition tendencies of a light Malaysian crude oil and the wax inhibiting potential of five different surfactants and their blends with SiO₂ nanoparticles. The surfactants used in this study were sophorolipid, 3-octyl-heptamethyl trisiloxane, 3-2-methoxyethoxy propyl-methyl-bis trimethylsilyloxy silane, 2-methoxy(polyethyleneoxy)propyl heptamethyltrisiloxane, and trimethylene-1,3-bis hexadecyl dimethylammonium bromide, denominated by the authors as S1, S2, S3, S4, and S5, respectively. The screening results showed a significant influence on the paraffin inhibition efficiency on a wax deposition by using 400 mg·L⁻¹ of the surfactants diluted in water, achieving a reduction of 17.4, 34.9, 53.9, 51.2, and 45.6% on the amount of wax deposited by using surfactants S1, S2, S3, S4, and S5, respectively. Nevertheless, a further investigation demonstrated that by blending the surfactants with 1 wt % of a nanofluid (prepared with xylene and 400 mg·L⁻¹ of SiO₂ nanoparticles), the wax deposition decreased up to 63.4, 64.8, 81.4, 73.1, and 55.9% for the crude oil in the presence of S1, S2, S3, S4, and S5 surfactants, respectively, revealing the exceptional ability of the nanoparticles for

inhibiting wax deposition.⁵⁵ Hussein et al.⁵⁸ studied the influence of several types of nanoparticles on the rheological behavior and wax content of model oils, including Fe₂O₃, ZnO, and MgO nanomaterials. From the study, the addition of 1000 mg·L⁻¹ of ZnO nanoparticles with particle sizes of 10.37 and 16.37 nm to the crude oil reduced wax deposition by 27.18 and 49.83, respectively. Wang et al.⁵⁹ studied the effect of nanocomposite PPDs (NPPDs), composed of modified nano-montmorillonite with ethylene/vinyl acetate, on the wax deposition behavior via a cold finger (CF) test. It was found that the addition of NPPDs, at concentrations of 50, 100, and 200 mg·L⁻¹, lowers the wax deposition by up to 39.39%.

Despite the progress in the implementation of nanotechnology for wax inhibition/deposition, the mechanisms of how nanoparticles affect wax crystallization and how nanoparticles can enhance the performance of conventional wax inhibitor systems are still unclear.⁴⁴ Previously, experiences with the nano-based inhibitors have been applied primarily as PPDs and yield point depressants to facilitate gelled pipeline restart. Therefore, reducing wax deposition rates is an important application for the nano-based wax inhibitors. In this sense, there is a huge interest in reducing wax deposition rates for the new nano-based wax inhibitors because most of the wax deposition issues at surface conditions take place at temperatures near the WAT. For this, a comprehensive study of the role of the nanoparticles is required in the inhibition of wax deposition and the mechanism that takes place during the wax inhibitor–nanoparticle–wax crystal interactions. Besides, the application of nanotechnology in wax inhibition issues under field conditions requires an extensive evaluation of the synergy among the carried fluid, the nanoparticles, and the optimization of the nanoparticle/carrier fluid ratio. To the best of our knowledge, research about how nanoparticles can enhance the performance of the commercial wax inhibitor in the reduction of wax deposition has not been reported yet. Therefore, the main objective of this study is to evaluate the synergistic effect of nanomaterials to improve the performance of chemical wax inhibitors to inhibit wax crystallization. Due to SiO₂ nanoparticles having been extensively evaluated with encouraging results, SiO₂-based nanofluids were developed aimed to obtain information about the mechanism that affects the wax inhibition when the nanoparticles are added to commercial wax inhibitor treatments.

This study provides several bench-top tests applied to the reduction of wax deposition for the selection of the most suitable nanoWT. Finally, the performance of the best nanoWT was evaluated using a flow loop test under representative field conditions such as temperature, pressure, and flow regime. Hence, the current research manuscript is both timely and essential to the flow assurance discipline. First, the treatments were added to WC oil at dosages from 5000 to 50,000 mg·L⁻¹ to observe remarkable differences in the behavior of the treatments. Differential scanning calorimetry (DSC) experiments and CF tests were carried out to study the effect of the WT on WAT and the wax inhibition efficiency (WIE) in a scenario with temperatures difference. The nanofluids were prepared by the addition of SiO₂ nanoparticles for concentrations from 100 to 500 mg·L⁻¹, and the prepared nanofluid was added at 5000 mg·L⁻¹. The most important findings are related to the role of the nanoparticle dispersion in the performance of the nanoWT system, showing an outstanding synergistic effect in the wax inhibition perform-

ance when the nanoparticles are highly dispersed. An outstanding relationship between the WAT and the WIE indicates that the modification of the wax crystallization process and crystal structure determines the inhibition efficiency. Otherwise, valuable results were obtained using Poiseuille's law for the laminar regime and the pressure drop data when the crude oil is flowing in the absence and presence of nanoWT during the flow loop test as an approximation of the overall deposit thickness during the experiment. This study provides a landscape of the use of nanomaterials for inhibition of paraffin wax deposition and their contribution to increasing productivity and profitability of oil wells due to the reduction of plugging of the production pipeline.

2. MATERIALS AND METHODS

2.1. Materials. Hydrophilic fumed SiO₂ nanoparticles with a specific surface area of 380 m²·g⁻¹ were supplied by Evonik Industries AG (Aerosil 380, Evonik Industries Co., Essen, Germany). Two commercial wax inhibitor treatments were kindly provided for companies A and B, and wax inhibitor treatments were labeled as WT1 and WT2, respectively. According to the operator company, co-polymerized ethylene wax inhibitor polymers are the main component of the formulations. However, insufficient information was provided about the polymer type and the overall treatment composition due to the non-disclosure agreement (NDA) signed with them. Physicochemical properties such as density, surface tension, viscosity, and conductivity for WT1 and WT2 are 0.95 and 0.96 mg·L⁻¹, 26.1 and 24.1 mN·m⁻¹, 4.13 and 11.05 cP, and 4.5 and 5.5 mS·cm⁻¹, respectively.

A WC oil sample from a reservoir located in the eastern of Colombia with a specific gravity of 42.7°API was used in this study. The WC oil viscosity is 2.3 cP at 30 °C and saturates, aromatics, resins, and asphaltenes content of 64.59, 18.89, 16.47, and 0.05% in mass fraction, respectively. In addition, the wax content of the crude oil is 12.3% in mass fraction. It is worth mentioning that the production reports for the oil reservoir confirm severe wax deposition in surface facilities and transportation lines, suggesting high issues induced by wax precipitation and deposition.

2.2. Wax Inhibitor Treatment Characterization. Wax inhibitor treatments were characterized through Fourier transform infrared (FTIR) spectroscopy analysis. Besides, the measurement of physicochemical parameters such as density, viscosity, surface tension, and conductivity were accomplished. FTIR spectra of the WTs were obtained using an IRAffinity 1-S spectrometer (Shimadzu Corporation, Japan), using 2-propanol as the standard liquid at atmospheric conditions.⁶⁰ For this, 10 sweeps per minute were taken at the wavelength range from 600 to 4500 cm⁻¹ with a resolution of 1 cm⁻¹. Density measurements were achieved using a pycnometer device based on the standard ASTM D891-18.⁶¹ Surface tension was obtained using the Du Nouy ring method in an Attention Sigma 702 (Biolin Scientific, ESPOO, Uusimaa, Finland) device. Furthermore, a multiparameter device Orion Star A215 (Thermo Scientific, USA) was used for the measurement of the electrical conductivity of the WTs. Finally, the viscosity of the samples was obtained by a rotational viscometer VL100003 (Fungilab, Barcelona, Spain).

2.3. Wax Inhibition Experiments. In this section, several techniques including DSC and CF tests were performed to the evaluation of the commercial WT in the absence and presence of SiO₂. DSC experiments were employed for the study of the

effect of the treatment nature in the alteration of the WAT. Then, at the best concentration for both WTs, the effect of SiO₂ was evaluated ranging the nanoparticle concentration between 0 and 500 mg·L⁻¹ in the WT (NanoWT) solution using both DSC and CF experiments. Finally, at the selected nanoparticle concentration, the effect of the NanoWT concentration in the WC oil was performed for nanofluid dosages from 20 to 5000 mg·L⁻¹. Before any of the proposed tests were performed, the crude oil in the absence/presence of WT/NanoWT was heated at 40 °C at a constant stirring of 300 rpm for 12 h to eliminate any thermal and mechanical history of the crude oil.

2.3.1. DSC Experiments. DSC experiments were achieved on a Q2000 differential scanning calorimeter (TA Instruments, Inc., New Castle, DE, USA) with hermetically sealed aluminum pans. Almost 30 mg of the WC oil in the absence and presence of the WT/NanoWT was subjected to a temperature sweep ranging from 60 to -20 °C at a fixed cooling rate of 1 °C·min⁻¹.^{44,62} It is worth mentioning that the WAT is evidenced by a sharp increase in the exothermic heat flow signal.⁵² Supporting Information shows the calorimetric curves for the WC oil in the absence and presence of WT and NanoWT systems and provides information about the method used in the current manuscript.

2.3.2. CF Test. Commonly, the wax inhibitor performance is evaluated using a CF device which consists of a thermal bath where the WC oil is immersed to keep the crude oil temperature above the WAT (T_{bulk}) at constant stirring. A U-shaped metal surface is inserted into the bulk oil with cold water circulating. To keep the temperature below the bulk oil temperature (T_{surface}) within it, it induces the wax deposition in the metal surface due to the temperature gradient inside the bulk solution.^{53,55,63,64} The schematic representation of the CF device is shown in Figure 1.

Almost 300 mL of the WC oil in the absence/presence of WT/NanoWT is conditioned at $T_{\text{bulk}} = 30$ °C for 1 h at 300 rpm to solubilize the unstable wax and to remove any thermal history before. Then, a U-shaped metal with cold water circulating at $T_{\text{surface}} = 5$ °C was immersed in the bulk solution

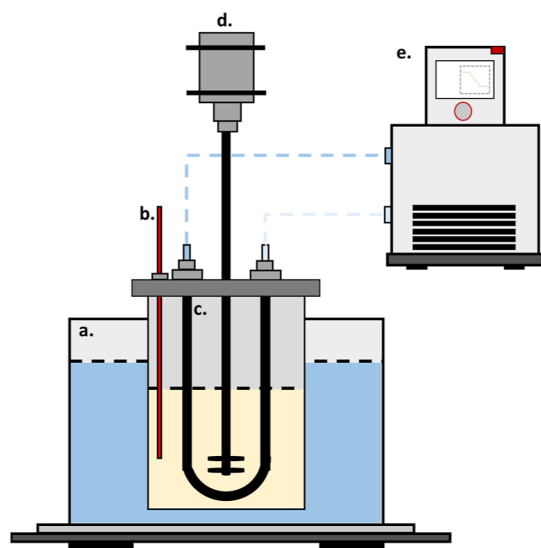


Figure 1. Schematic representation of a CF apparatus. (a) Heating water bath, (b) thermometer, and (c) U-tube CF. Inner diameter: 0.6 cm (d) impeller and (e) chiller.

for 4 h. Finally, the wax deposit was collected from the U-shaped metal surface and weighed to estimate the WIE according to the equation proposed by Bello et al.⁶⁵

$$\text{WIE} = \frac{W_f - W_t}{W_f} \times 100 \quad (1)$$

whereas W_f (g) is the amount of wax deposited before the addition of WT/NanoWT and W_t (g) is the amount of wax deposited after the addition of WT/NanoWT systems.

2.4. Flow Loop Experiments. The flow loop device consists of a storage and disposal tank connected by stainless-steel pipeline where the WC oil flows at a constant flow rate provided by a gear pump. A schematic representation of the flow loop system is shown in Figure 2. The dynamic test was conducted based on the field conditions where the WCO sample was extracted. According to the information provided by the operator company, the major wax deposit problems were identified in the entry of the field tank battery, so the current crude oil flow (19,000 barrels per day) was scaled up to a suitable laboratory condition to have a proper representation of the flow regime in the field. The test section has a length of 60 cm composed of an inner pipe with an internal diameter of 1.6 mm and an outer pipe with an inner diameter of 6.4 mm. In the inner pipe, the WC oil is circulating, while in the annulus, a glycol/water mixture acting as a coolant at a temperature of 5 °C system is flowing in the opposite direction to maintain the temperature in the test section during the experiments. For each experiment, the WC oil is first heated and stirred for 12 h at 30 °C to remove any thermal history and then poured into the feeding holder. Then, the oil is pumped into the flow loop through the test section and returned to a disposal holder at a volumetric flow rate of 247.8 cm³·min⁻¹. The difference in the pressure during the experiments was recorded and used for the evaluation of the nanofluid performance and the calculation of the deposit thickness.

The flow loop experiments can be divided into three scenarios: (i) baseline, (ii) deposition, and (iii) inhibition. In the first scenario, the crude oil is pumped at a temperature of 30 °C which is over the crude oil WAT value. In the damage step, the crude oil is pumped at a temperature of 16 °C which is lower than the WAT value, so wax aggregation and deposition in the pipe wall surface are expected. Before the inhibition stage, the deposit in the test section was washed with methyl ethyl ketone (MEK) to remove any excess wax remaining on the pipe wall. Then, the air is flowed through the test section at a high flow rate to remove the MEK in the device. In the inhibition scenario, the crude oil is mixed with the selected NanoWT at the desired nanofluid concentration and then pumped at a 16 °C.

3. RESULTS AND DISCUSSION

3.1. Wax Inhibitor Treatment Characterization. Figure 3 shows the IR spectra obtained for WT1 and WT2. In general, both treatments show a similar band with varied intensity, suggesting more or low presence for each identified functional group. Hydroxy groups (O–H) can be identified in both treatments due to the stretch vibration at a wavelength from 3500 to 3200 cm⁻¹ and the bend vibration between 1440–1395 and 950–910 cm⁻¹.^{66,67} In this sense, it can be inferred that WT2 exhibits more O–H groups, which could be linked to a higher presence of water- and/or alcohol-based

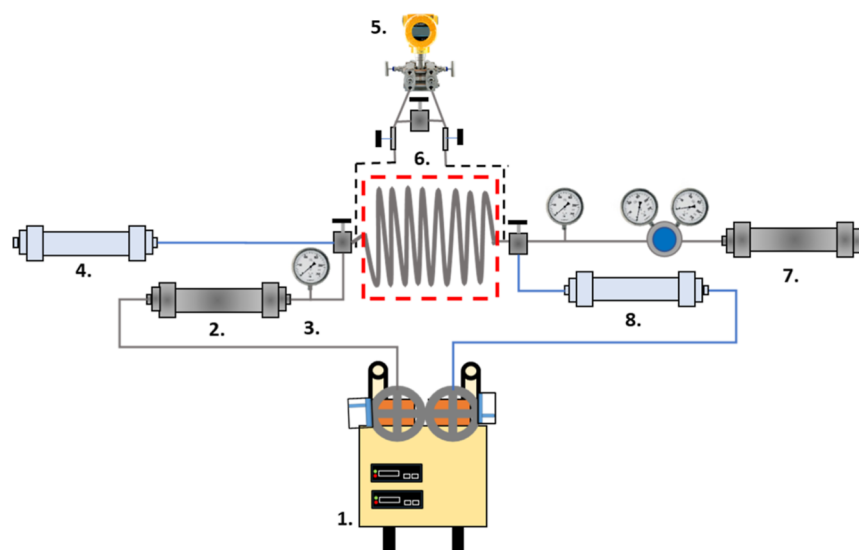


Figure 2. Schematic representation of the flow loop experiment for wax deposition: (1) positive displacement pump, (2) crude oil feeding holder, (3) manometer, (4) coolant disposal holder, (5) differential pressure transducer, (6) test section, (7) crude oil disposal holder, and (8) coolant feeding holder.

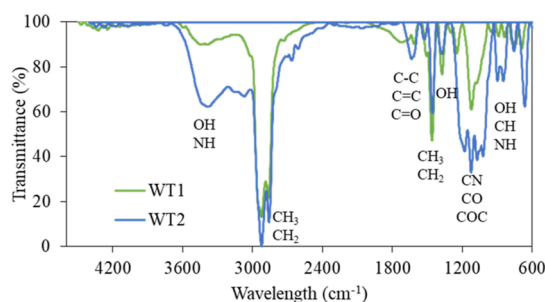


Figure 3. FTIR spectra of received commercial wax inhibitor treatments.

compounds in its formulation. Otherwise, C–H and C–C have been identified due to stretch vibration from 3000–2850 to 1500–1400 cm^{-1} , respectively, suggesting the presence of hydrocarbon compounds in the formulation in both WT1 and WT2. Besides, C–C (in-ring) stretch vibration from 1600–1585 to 1500–1400 cm^{-1} indicates that some of the hydrocarbons are composed of aromatic rings, typically found in WT systems.^{68,69} Other functional groups displayed by both inhibitors are the stretching of N–H, C–O, C–N, and C=C between 3400–3300, 1124–1087, 1250–1020, and 995–905 cm^{-1} , respectively.^{70–72} In conclusion, it is inferred that both commercial inhibitors are prepared with organic compounds as the major carried fluid, but WT2 displays the presence of more water- and/or alcohol-based compounds than WT1.

3.2. Effect of the WT Concentration. Figure 4 shows the effect of the WT concentration in the modification of the crude oil WAT. WC oil has a WAT value of 25.35 °C, which is a typical value for crude oil with wax deposition issues.^{73,74} When WT1 is added to crude oil for concentrations between 5000 and 50,000 $\text{mg}\cdot\text{L}^{-1}$, it is observed that the treatment can reduce the WAT to 24.68 °C at 5000 $\text{mg}\cdot\text{L}^{-1}$, which correspond to a reduction of 2.6%. However, when the concentration of WT1 is raised, there is no effect of the treatment in the reduction of the WAT. In the case of WT2, there is a reduction in the WAT number for all the

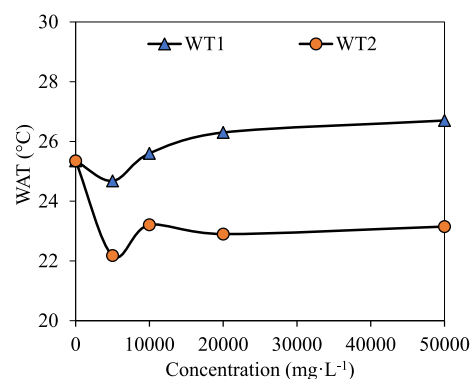


Figure 4. WAT of WC in the absence and presence of WT1 and WT2 at concentrations from 5000 to 50,000 $\text{mg}\cdot\text{L}^{-1}$.

concentrations. In this sense, WT2 added at 5000, 10,000, 20,000, and 50,000 $\text{mg}\cdot\text{L}^{-1}$ exhibits reductions in the WAT value of 12.5 (22.18 °C), 8.4 (23.21 °C), 9.7 (22.9 °C), and 8.7% (23.15 °C), respectively. According to the results, the best behavior for both treatments was found at 5000 $\text{mg}\cdot\text{L}^{-1}$; therefore, CF experiments were conducted at the same concentration.

The estimation of WIE for the WC oil in the presence of WT1 and WT2 at 5000 $\text{mg}\cdot\text{L}^{-1}$ is displayed in Figure 5. The addition of the WT reveals WIE values of 31.0 and 52.1% for WT1 and WT2, respectively. The results are in agreement with Bello et al.,⁶⁹ who evaluate the influence of chemical-based treatments on the inhibition of wax deposition. The results have shown that the addition of MEK, cyclohexanone, trichloroethylene, and xylene, added at 10,000 $\text{mg}\cdot\text{L}^{-1}$ to the crude oil, reduce the deposited wax in 26.0, 44.0, 82.0, and 74.0%, respectively. Besides, the obtained WIE can be correlated with the WAT values, whereas a higher reduction in the WAT means higher wax inhibition.⁷⁵

3.3. Effect of the Nanoparticle Concentration in NanoWT. Figure 6 shows the effect of the addition of SiO_2 nanomaterials on WT1 and WT2 in the WAT values for prepared WC oil in the presence of both treatments at 5000

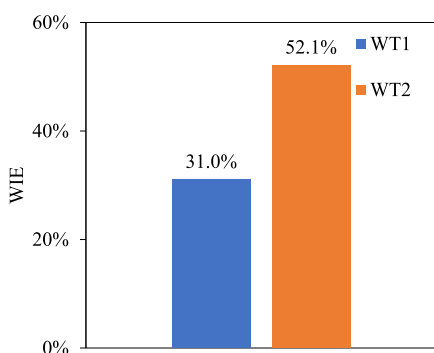


Figure 5. WIE of WT1 and WT2 in the CF test at a treatment concentration of 5000 mg·L⁻¹.

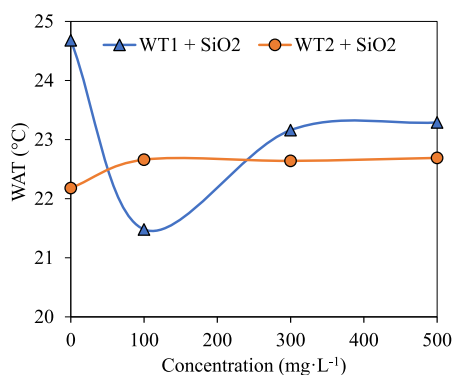


Figure 6. WAT of WC in the presence of NanoWT1 and NanoWT2 at nanoparticle concentrations from 0 to 500 mg·L⁻¹. Nanofluid dosage in WC: 5000 mg·L⁻¹.

mg·L⁻¹. In the presence of SiO₂ nanoparticles, WT1 exhibits a sharp reduction in the WAT value with a decrease of 15.0% at a nanoparticle dosage of 100 mg·L⁻¹. Besides, the addition of the nanoparticles at 300 and 500 mg·L⁻¹ reveals reductions of 8.6 and 8.1%, respectively, suggesting that the addition of nanoparticles is effective especially high at low nanoparticle dosage. Low nanoparticle concentration guarantees high dispersion and hence superior availability of surface-active sites for the interaction of the wax fractions within the nanomaterials.⁷⁶ The increase in the nanoparticle concentration is associated with an increase in the particle packing factor causing nanoparticle aggregation and reducing the interaction energy among the wax crystals.⁷⁷ The aggregation of nanoparticles leads to a reduction in the effective surface area of the nanomaterials and thus affects the interaction with the wax crystals, showing no improvement in the WAT value. Otherwise, in the case of WT2, a reduction in the effectiveness of the treatment is observed, whereas nanoparticle dosages of 100, 300, and 500 mg·L⁻¹ showed an increase in the WAT value of 2.2, 2.1, and 2.3%, respectively, which could be related with aggregation phenomena. In this sense, the interactions between the WT-based compounds with SiO₂ nanoparticles that affect the nanoparticle dispersion determine the performance of the nanoWT. Low nanoparticle dispersion leads to a reduction in the effective surface area of the nanomaterials and thus affects the interaction with the wax crystals, showing no improvement in the WAT value. The nanoparticle dispersion degree in both WT was corroborated by zeta-potential (ζ) measurements. For this, ζ values of WT1 and WT2 in the presence of the nanoparticles at 100 mg·L⁻¹ have been conducted, showing superior nanoparticle stability in WT1

(-35.5 mV) than that in WT2 (-15.2 mV).⁷⁸ Weak intermolecular interactions between the WT2 and SiO₂ together with a higher viscosity for WT2 in comparison with WT1 led to a low nanoparticle dispersion degree, promoting the formation of large aggregates in the bulk solution.

To compare the WIE values of prepared NanoWT at the same nanoparticle concentration, CF tests were conducted by the preparation of NanoWT1 and NanoWT2 at a nanoparticle concentration of 100 mg·L⁻¹. In this sense, Figure 7 shows the

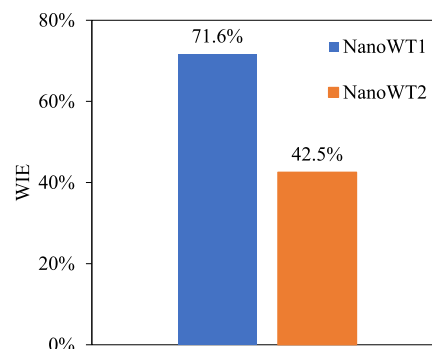


Figure 7. WIE of NanoWT1 and NanoWT2 in the CF test. Nanoparticle concentration in WT1 and WT2: 100 mg·L⁻¹. Nanofluid dosage in WC: 5000 mg·L⁻¹.

WIE in the CF test for the WC oil treated with NanoWT1 and NanoWT2 at a nanofluid dosage of 5000 mg·L⁻¹. The WIE values for NanoWT1 and NanoWT2 were 71.6 and 42.5%, showing that the interaction between the nanoparticles and the wax inhibitor affects the role of the nanofluid in the inhibition of the wax deposition. Ridzuan et al.⁵³ studied the behavior of a commercial PPD in the absence and presence of a clay-based nanomaterial on the wax deposition using a CF test device, showing that the nanoparticles can alter the wax crystal solubility in the crude oil. According to the author, the addition of nanoparticles in PPD systems improves the inhibition efficiency by 11% in comparison to the use of PPD in the absence of nanoparticles. Remarkable results have been obtained by Lim et al.,⁵⁵ who evaluate the combination of SiO₂ nanoparticles and several types of surfactants in a load ratio of 3:1 in the crude oil. In this study, the WIE value was increased from 53.9 to 81% with the addition of SiO₂ onto the best surfactant; however, the synergy between them is strongly dependent on the surfactant nature and the nanoparticle interactions. In the case of WT1, it is observed that the addition of SiO₂ increases the effectiveness of wax inhibition by 58.9% in comparison with the same system in the absence of nanoparticles (from 31.0 to 71.6%). These findings differ from the results obtained with WT2, where a reduction in effectiveness near 20% was detected (from 52.1 to 42.5%). Similar to the results obtained in DSC experiments, it can be inferred that the interactions between WT2 and SiO₂ affect the dispersion degree of the nanoparticles and hinder their role in the enhancement of wax inhibition.

3.4. Effect of the Nanofluid Concentration in WC. The addition of nanoparticles in the bulk solution of WT1 reveals a synergistic effect between the WT and the nanomaterials in the inhibition of the wax deposition; however, the results were not convincing for WT2. For this reason, Figure 8 shows the effect of the concentration of NanoWT1 in the WC oil in the WAT number for a prepared nanofluid with a nanoparticle dosage of 100 mg·L⁻¹. It can be observed that the increase in the

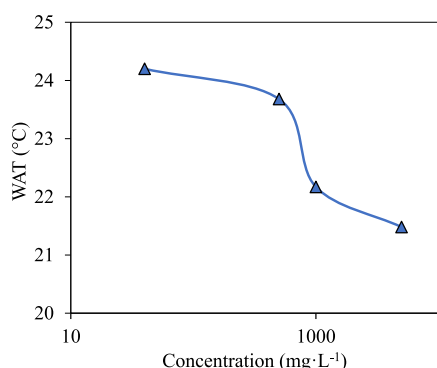


Figure 8. WAT of WC in the presence of NanoWT1. Nanoparticle concentration: 100 mg·L⁻¹. Nanofluid dosage in WC: 40–5000 mg·L⁻¹.

nanofluid concentration will lead to an improvement in the reduction of WAT value. In this respect, improvement of 4.5, 6.7, 12.5, and 15.3% was found at nanofluid dosages of 40, 500, 1000, and 5000 mg·L⁻¹, revealing a sustained reduction in the WAT for concentrations from 500 to 1000 mg·L⁻¹. Due to the low concentration of nanoparticles in WT, a high dispersion of the nanomaterials in the bulk solution is expected, so an increase in the nanofluid concentration will lead to an increase in the availability of surface-active functional groups for the wax crystal adsorption.

The effect of the NanoWT1 concentration on the WIE is displayed in Figure 9. Panel (a) from Figure 9 shows that the increase in the nanofluid dosage led to an improvement in the WIE value. Even the maximum WAT reduction is close to

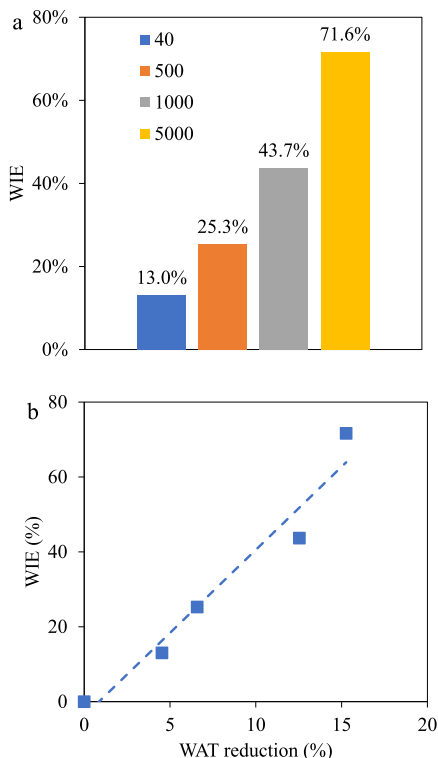


Figure 9. (a) WIE of NanoWT1 in the CF test. Nanoparticle concentration in WTF: 100 mg·L⁻¹. Nanofluid dosage in WC: 40–5000 mg·L⁻¹. (b) WIE as a function of the WAT reduction for prepared WC oils in the presence of NanoWT1.

15.3% in comparison with the crude oil in the absence of selected WT, the effect of the nanofluid incorporation is observed due to a clear reduction in the deposited wax during the CF experiments, suggesting that the role of the nanofluid in the wax inhibition is related to the modification of the solubility and morphology of the wax crystals that affect the stability of the wax molecules from temperatures between the crystallization and the gelation temperature. In this sense, panel (b) from Figure 9 shows the relationship between the reduction in the WAT and the increase of the efficiency in the inhibition of wax deposition.

For the selection of the NanoWT1 concentration during the flow loop test, the economic criterion has been considered, where low WT concentrations are highly recommended.^{79,80} Concentrations from 40 to 500 mg·L⁻¹ are attractive because the obtained WIE percentage is from 13 to 25%. In this sense, NanoWT1 will be employed at a dosage of 200 mg·L⁻¹ during the inhibition process in the flow loop experiments.

3.5. Flow Loop Experiments. Figure 10 displays the obtained results in the flow loop experiments during the

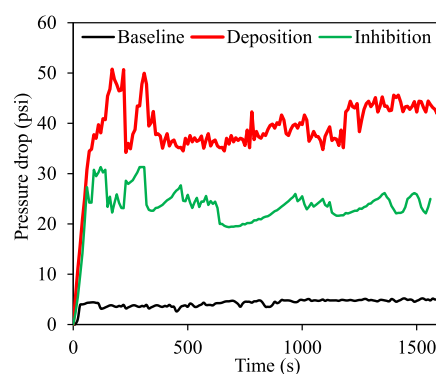


Figure 10. Pressure drops as a function of time.

baseline, wax deposition, and wax inhibition stages. During the baseline stage, the injection of the WC oil at 30 °C led to an average pressure drop of 4.2 psi. However, when the crude oil temperature falls to 16 °C, the average pressure drop in the deposition scenario is 34.6 psi. Considering that both temperatures in baseline and deposition stages are above and below the WAT value, respectively, an increase by 8.2 times in the pressure drop suggests the formation of wax deposits in the pipeline surface.⁸¹ In the inhibition stage, the addition of NanoWT1 at 200 mg·L⁻¹ in the crude oil before use led to a pressure drop of 23.6 psi, which is 1.5 times the pressure drops in comparison with the baseline stage. In contrast with the deposition stage, the pressure drop during the inhibition scenario was reduced by 31.8%, revealing a superior performance of the NanoWT1 in the inhibition of the wax aggregation and subsequent deposition on the wall surface.

The CF test and flow loop experiments reveal a relationship between the performance of the nanoWT1 in both static and dynamic tests in terms of the nanofluid capacity to inhibit the wax deposition and hence to improve the flow assurance during the loop experiments. However, there are quite different shear regimes and temperature gradients that make a clear relationship difficult between both tests. Further studies are necessary to have a deeper correlation between CF and flow loop results under comparable temperature and shear conditions.⁸²

4. CONCLUSIONS

A comprehensive study of the effect of the incorporation of SiO₂ in commercial WT has been developed in the present study. For this, DSC and CF tests were carried out to obtain information about the role of the nanoparticles in the inhibition of wax deposition toward the modification of WAT and the improvement of the WIE. In this sense, in the absence of the nanomaterials, WT1 and WT2 at 5000 mg·L⁻¹ show a reduction in the WAT and increase in the WIE of 2.6 and 31.0% for WT1 and 12.5 and 52.1% for WT2, respectively. A clear synergy in the wax inhibition process is displayed between the WT1 and SiO₂ nanoparticles at 100 mg·L⁻¹ because the WAT was reduced by 15% and WIE was increased by 40.6%. However, NanoWT₂ with SiO₂ nanoparticles at 100 mg·L⁻¹ shows an increase of 2.2% in the WAT, and WIE was reduced by 9.6%. The interactions between the WT-based compounds with SiO₂ nanoparticles that affect the nanoparticle dispersion determine the performance of the nanoWT. Weak intermolecular interactions between the WT2 and SiO₂ together with a higher viscosity for WT2 in comparison with WT1 led to a low nanoparticle dispersion degree, promoting the formation of large aggregates in the bulk solution. Finally, the best nanoWT was evaluated in a flow loop test under representative field conditions such as temperature, pressure, and flow regime. The flow loop experiments of the WC oil below and above the WAT value show the high tendency of the crude oil to induce the clogging of the pipe surface. The pressure drop data show an increase of 8.3 times the pressure drops when the crude oil is injected at a temperature below the WAT value. Nevertheless, when NanoWT1 is added to the crude oil at a nanofluid concentration of 200 mg·L⁻¹, the pressure drop is 1.5 times the baseline pressure drops and 31.8% lower than the pressure drop exhibited in the deposition scenario. These findings suggest that the implementation of the nanotechnology for the improvement of wax inhibition is strongly dependent on the dispersion degree of the nanomaterials and hence the availability of surface-active functional groups.

■ ASSOCIATED CONTENT

SI Supporting Information

The Supporting Information is available free of charge at <https://pubs.acs.org/doi/10.1021/acsomega.3c00802>.

Methodology for DSC experiments; DSC curves for the WC oil in the absence of wax inhibitor treatments; DSC curves for the WC oil in the presence of WT1 and WT2; WT concentrations from 5000 to 50,000 mg·L⁻¹; DSC curves for the WC oil in the presence of NanoWT1 and NanoWT2 at nanoparticle concentrations from 0 to 500 mg·L⁻¹; nanofluid dosage in WC: 5000 mg·L⁻¹; DSC curves for the WC oil in the presence of NanoWT1; nanoparticle concentration: 100 mg·L⁻¹; and nanofluid dosage in WC: 40–5000 mg·L⁻¹ (PDF)

■ AUTHOR INFORMATION

Corresponding Authors

Camilo A. Franco – Grupo de Investigación en Fenómenos de Superficie—Michael Polanyi, Departamento de Procesos y Energía, Facultad de Minas, Universidad Nacional de Colombia, Medellín 050034, Colombia; orcid.org/0000-0002-6886-8338; Email: cafrancoar@unal.edu.co

Farid B. Cortés – Grupo de Investigación en Fenómenos de Superficie—Michael Polanyi, Departamento de Procesos y Energía, Facultad de Minas, Universidad Nacional de Colombia, Medellín 050034, Colombia; orcid.org/0000-0003-1207-3859; Email: fbcortes@unal.edu.co

Authors

Daniel López – Grupo de Investigación en Fenómenos de Superficie—Michael Polanyi, Departamento de Procesos y Energía, Facultad de Minas, Universidad Nacional de Colombia, Medellín 050034, Colombia

As A. Ríos – Grupo de Investigación en Fenómenos de Superficie—Michael Polanyi, Departamento de Procesos y Energía, Facultad de Minas, Universidad Nacional de Colombia, Medellín 050034, Colombia

Juan D. Marín – Departamento de Ingeniería, Gerencia de Desarrollo y Producción, Vicepresidencia Piedemonte, Ecopetrol SA CPF Floreña, Piedecuesta 681011, Colombia

Richard D. Zabala – Departamento de Tecnologías de Producción, Gerencia Centro Técnico de Desarrollo, Gerencia General de Desarrollo, Ecopetrol S.A, Bogotá 1021, Colombia

Jaime A. Rincon – Centro de Innovación y Tecnología ECOPETROL ICP, Bogota 1021, Colombia

Sergio H. Lopera – Grupo de Investigación en Yacimientos de Hidrocarburos, Departamento de Procesos y Energía, Facultad de Minas, Universidad Nacional de Colombia, Medellín 050034, Colombia

Complete contact information is available at:

<https://pubs.acs.org/10.1021/acsomega.3c00802>

Notes

The authors declare no competing financial interest.

■ ACKNOWLEDGMENTS

The authors acknowledge ECOPETROL S.A, Instituto Colombiano del Petróleo—ICP and Grupo de investigación en Fenómenos de Superficie Michael Polanyi (Universidad Nacional de Colombia) for the constant support and fruitful recommendations.

■ REFERENCES

- (1) Agency, I. E. *Electricity Market Report*; International Energy Agency <https://www.iea.org/>, January 2022, 2022.
- (2) Li, H.; Zhang, J.; Song, C.; Sun, G. The influence of the heating temperature on the yield stress and pour point of waxy crude oils. *J. Pet. Sci. Eng.* **2015**, *135*, 476–483.
- (3) Kumar, L.; Paso, K.; Sjöblom, J. Numerical study of flow restart in the pipeline filled with weakly compressible waxy crude oil in non-isothermal condition. *J. Non-Newtonian Fluid Mech.* **2015**, *223*, 9–19.
- (4) Chala, G. T.; Sulaiman, S. A.; Japper-Jaafar, A. Flow start-up and transportation of waxy crude oil in pipelines-A review. *J. Non-Newtonian Fluid Mech.* **2018**, *251*, 69–87.
- (5) Philp, R. P.; Bishop, A.; Del Rio, J.-C.; Allen, J. Characterization of high molecular weight hydrocarbons (> C40) in oils and reservoir rocks. *Geological Society, London, Special Publications* **1995**, *86*, 71–85.
- (6) Fahim, M. A.; Al-Sahhaf, T. A.; Elkilani, A. *Fundamentals of Petroleum Refining*; Elsevier, 2009.
- (7) Speight, J. G. *The Chemistry and Technology of Petroleum*; CRC Press, 2006.
- (8) Yao, B.; Li, C.; Yang, F.; Sjöblom, J.; Zhang, Y.; Norrman, J.; Paso, K.; Xiao, Z. Organically modified nano-clay facilitates pour point depressing activity of polyoctadecylacrylate. *Fuel* **2016**, *166*, 96–105.

- (9) Chen, S.; Øye, G.; Sjöblom, J. Rheological properties of model and crude oil systems when wax precipitate under quiescent and flowing conditions. *J. Dispersion Sci. Technol.* **2007**, *28*, 1020–1029.
- (10) Mohyaldinn, M. E.; Husin, H.; Hasan, N.; Elmubarak, M.; Genefid, A.; Dheeb, M. Challenges during operation and shutdown of waxy crude pipelines. *Processing of Heavy Crude Oils—Challenges and Opportunities*; IntechOpen: Rijeka, Croatia, 2019; Vol. 153.
- (11) Edwards, R. Crystal habit of paraffin wax. *Ind. Eng. Chem.* **1957**, *49*, 750–757.
- (12) He, C.; Ding, Y.; Chen, J.; Wang, F.; Gao, C.; Zhang, S.; Yang, M. Influence of the nano-hybrid pour point depressant on flow properties of waxy crude oil. *Fuel* **2016**, *167*, 40–48.
- (13) Kurniawan, M.; Norrman, J.; Paso, K. Pour point depressant efficacy as a function of paraffin chain-length. *J. Pet. Sci. Eng.* **2022**, *212*, 110250.
- (14) Chouparova, E.; Lanzirrotti, A.; Feng, H.; Jones, K. W.; Marinkovic, N.; Whitson, C.; Philp, P. Characterization of petroleum deposits formed in a producing well by synchrotron radiation-based microanalyses. *Energy Fuels* **2004**, *18*, 1199–1212.
- (15) Theyab, M. A. Wax deposition process: mechanisms, affecting factors and mitigation methods. *Open Access J. Sci. Technol.* **2018**, *2*, 112–118.
- (16) Ajayi, O. E. *Modelling of Controlled Wax Deposition and Loosening in Oil and Gas Production Systems*; Institutt for Energi-og Prosessteknikk, 2013.
- (17) Rehan, M.; Nizami, A.-S.; Taylan, O.; Al-Sasi, B. O.; Demirbas, A. Determination of wax content in crude oil. *Pet. Sci. Technol.* **2016**, *34*, 799–804.
- (18) Singhal, H.; Sahai, G.; Pundeer, G.; Chandra, K. Designing and selecting wax crystal modifier for optimum field performance based on crude oil composition. *SPE Annual Technical Conference and Exhibition*; OnePetro, 1991.
- (19) Gong, J.; Zhang, Y.; Liao, L.; Duan, J.; Wang, P.; Zhou, J. Wax deposition in the oil/gas two-phase flow for a horizontal pipe. *Energy Fuels* **2011**, *25*, 1624–1632.
- (20) Matzain, A.; Apte, M. S.; Zhang, H.-Q.; Volk, M.; Brill, J. P.; Creek, J. Investigation of paraffin deposition during multiphase flow in pipelines and wellbores—part 1: experiments. *J. Energy Resour. Technol.* **2002**, *124*, 180–186.
- (21) Matzain, A. *Multiphase Flow Paraffin Deposition Modeling*; The University of Tulsa, 2000.
- (22) Rittirong, A.; Panacharoensawad, E.; Sarica, C. Experimental study of paraffin deposition under two-phase gas/oil slug flow in horizontal pipes. *SPE Prod. Oper.* **2017**, *32*, 99–117.
- (23) Couto, G. H.; Chen, H.; Dellecase, E.; Sarica, C.; Volk, M. An investigation of two-phase oil/water paraffin deposition. *SPE Prod. Oper.* **2008**, *23*, 49–55.
- (24) Bordalo, S. N.; Oliveira, R. D. Experimental study of oil/water flow with paraffin precipitation in submarine pipelines. *SPE Annual Technical Conference and Exhibition*; OnePetro, 2007.
- (25) Ragunathan, T.; Husin, H.; Wood, C. D. Wax formation mechanisms, wax chemical inhibitors and factors affecting chemical inhibition. *Appl. Sci.* **2020**, *10*, 479.
- (26) Southgate, J. *Wax Removal Using Pipeline Pigs*; Durham University, 2004.
- (27) Singh, P.; Venkatesan, R.; Fogler, H. S.; Nagarajan, N. R. Morphological evolution of thick wax deposits during aging. *AIChE J.* **2001**, *47*, 6–18.
- (28) Venkatesan, R.; Östlund, J.-A.; Chawla, H.; Wattana, P.; Nydén, M.; Fogler, H. S. The effect of asphaltenes on the gelation of waxy oils. *Energy Fuels* **2003**, *17*, 1630–1640.
- (29) Machado, A. L. d. C.; Lucas, E. F. Poly (ethylene-co-vinyl acetate)(EVA) copolymers as modifiers of oil wax crystallization. *Pet. Sci. Technol.* **1999**, *17*, 1029–1041.
- (30) Ruwoldt, J.; Humborstad Sørland, G.; Simon, S.; Oschmann, H.-J.; Sjöblom, J. Inhibitor-wax interactions and PPD effect on wax crystallization: New approaches for GC/MS and NMR, and comparison with DSC, CPM, and rheometry. *J. Pet. Sci. Eng.* **2019**, *177*, 53–68.
- (31) Paso, K.; Senra, M.; Yi, Y.; Sastry, A.; Fogler, H. S. Paraffin polydispersity facilitates mechanical gelation. *Ind. Eng. Chem. Res.* **2005**, *44*, 7242–7254.
- (32) Clarke, E. W. Crystal types of pure hydrocarbons in the paraffin wax range. *Ind. Eng. Chem.* **1951**, *43*, 2526–2535.
- (33) Speight, J. G. *Fouling in Refineries*; Gulf Professional Publishing, 2015.
- (34) Haindade, Z.; Bihani, A. D.; Javeri, S.; Jere, C. In Enhancing flow assurance using Co-Ni nanoparticles for dewaxing of production tubing. *SPE international oilfield nanotechnology conference and exhibition*; OnePetro, 2012.
- (35) Aarseth, F. Use of electrical power in control of wax and hydrates. *Offshore Technology Conference*; OnePetro, 1997.
- (36) McClafflin, G.; Whitfill, D. Control of paraffin deposition in production operations. *J. Pet. Technol.* **1984**, *36*, 1965–1970.
- (37) Groffe, D.; Groffe, P.; Takhar, S.; Andersen, S. I.; Stenby, E. H.; Lindeloff, N.; Lundgren, M. A wax inhibition solution to problematic fields: A chemical remediation process. *Pet. Sci. Technol.* **2001**, *19*, 205–217.
- (38) Elochukwu, O. H.; Saaid, I. M.; Pilus, R. M. Organic deposit remediation using environmentally benign solvents: a review. *ARPN J. Eng. Appl. Sci.* **2014**, *9*, 1930–1935.
- (39) Ferworn, K. A.; Hammami, A.; Ellis, H. Control of wax deposition: an experimental investigation of crystal morphology and an evaluation of various chemical solvents. *International Symposium on Oilfield Chemistry*; OnePetro, 1997.
- (40) Etoumi, A. Microbial treatment of waxy crude oils for mitigation of wax precipitation. *J. Pet. Sci. Eng.* **2007**, *55*, 111–121.
- (41) Al-Yaari, M. Paraffin wax deposition: mitigation & removal techniques. *SPE Saudi Arabia section Young Professionals Technical Symposium*; OnePetro, 2011.
- (42) Makwashi, N.; Zhao, D.; Abdulkadir, M.; Ahmed, T.; Muhammad, I. Study on waxy crudes characterisation and chemical inhibitor assessment. *J. Pet. Sci. Eng.* **2021**, *204*, 108734.
- (43) Hao, L. Z.; Al-Salim, H. S.; Ridzuan, N. A Review of the Mechanism and Role of Wax Inhibitors in the Wax Deposition and Precipitation. *Pertanika J. Sci. Technol.* **2019**, *27*, 499.
- (44) Vakili, S.; Mohammadi, S.; Mirzaei Derazi, A.; Mahmoudi Alemi, F.; Hayatizadeh, N.; Ghanbarpour, O.; Rashidi, F. Effect of metal oxide nanoparticles on wax formation, morphology, and rheological behavior in crude oil: An experimental study. *J. Mol. Liq.* **2021**, *343*, 117566.
- (45) Jafari Ansaroudi, H.; Vafaie-Sefti, M.; Masoudi, S.; Behbahani, T. J.; Jafari, H. Study of the morphology of wax crystals in the presence of ethylene-co-vinyl acetate copolymer. *Pet. Sci. Technol.* **2013**, *31*, 643–651.
- (46) Soni, H. P.; Agrawal, K.; Agrawal, K.; Nagar, A.; Bharambe, D. Designing maleic anhydride- α -olifin copolymeric combs as wax crystal growth nucleators. *Fuel Process. Technol.* **2010**, *91*, 997–1004.
- (47) Ahmed, S. M.; Khidr, T. T.; Ismail, D. A. Effect of gemini surfactant additives on pour point depressant of crude oil. *J. Dispersion Sci. Technol.* **2018**, *39*, 1160–1164.
- (48) Coto, B.; Martos, C.; Espada, J. J.; Robustillo, M. D.; Pena, J. L. Experimental study of the effect of inhibitors in wax precipitation by different techniques. *Energy Sci. Eng.* **2014**, *2*, 196–203.
- (49) Machado, A. L.; Lucas, E. F.; González, G. Poly (ethylene-co-vinyl acetate)(EVA) as wax inhibitor of a Brazilian crude oil: oil viscosity, pour point and phase behavior of organic solutions. *J. Pet. Sci. Eng.* **2001**, *32*, 159–165.
- (50) Huang, Z.; Zheng, S.; Fogler, H. S. *Wax Deposition: Experimental Characterizations, Theoretical Modeling, and Field Practices*; CRC Press, 2016.
- (51) Marie, E.; Chevalier, Y.; Eydoux, F.; Germanaud, L.; Flores, P. Control of n-alkanes crystallization by ethylene-vinyl acetate copolymers. *J. Colloid Interface Sci.* **2005**, *290*, 406–418.
- (52) Yang, F.; Paso, K.; Norrman, J.; Li, C.; Oschmann, H.; Sjöblom, J. Hydrophilic nanoparticles facilitate wax inhibition. *Energy Fuels* **2015**, *29*, 1368–1374.

- (53) Ridzuan, N.; Subramanie, P.; Uyop, M. Effect of pour point depressant (PPD) and the nanoparticles on the wax deposition, viscosity and shear stress for Malaysian crude oil. *Pet. Sci. Technol.* **2020**, *38*, 929–935.
- (54) Song, X.; Yin, H.; Feng, Y.; Zhang, S.; Wang, Y. Effect of SiO₂ nanoparticles on wax crystallization and flow behavior of model crude oil. *Ind. Eng. Chem. Res.* **2016**, *55*, 6563–6568.
- (55) Lim, Z. H.; Al Salim, H. S.; Ridzuan, N.; Ngeue, R.; Sasaki, K.; Sasaki, K. Effect of surfactants and their blend with silica nanoparticles on wax deposition in a Malaysian crude oil. *Pet. Sci.* **2018**, *15*, 577–590.
- (56) Wijayanto, T.; Kurihara, M.; Kurniawan, T.; Muraza, O. Experimental investigation of aluminosilicate nanoparticles for enhanced recovery of waxy crude oil. *Energy Fuels* **2019**, *33*, 6076–6082.
- (57) Wang, F.; Zhang, D.; Ding, Y.; Zhang, L.; Yang, M.; Jiang, B.; Zhang, S.; Ai, M.; Liu, G.; Zhi, S.; et al. The effect of nanohybrid materials on the pour-point and viscosity depressing of waxy crude oil. *Chin. Sci. Bull.* **2011**, *56*, 14–17.
- (58) Che Mohamed Hussein, S. N.; Dollah, A.; Mohamad Salleh, M. F.; Othman, N. H.; Che Abdul Rahim, A. N.; Japperi, N. S. Synthesis of ZnO Nanoparticles for Wax Deposition Control and Oil Upgrading: Effect of Ratio of Zinc Acetate Dihydrate to Oxalic Acid Dihydrate. In *Key Engineering Materials*; Trans Tech Publications, 2019; pp 411–420.
- (59) Wang, C.; Zhang, M.; Wang, W.; Ma, Q.; Zhang, S.; Huang, H.; Peng, Z.; Yao, H.; Li, Q.; Ding, Y.; et al. Experimental Study of the Effects of a Nanocomposite Pour Point Depressant on Wax Deposition. *Energy Fuels* **2020**, *34*, 12239–12246.
- (60) López, D.; Zabala, R. D.; Matute, C.; Lopera, S. H.; Cortés, F. B.; Franco, C. A. Well injectivity loss during chemical gas stimulation process in gas-condensate tight reservoirs. *Fuel* **2021**, *283*, 118931.
- (61) ASTM D95-13. *Standard Test Method for Water in Petroleum Products and Bituminous Materials by Distillation*; ASTM International: West Conshohocken, PA, 2018.
- (62) Norrman, J.; Solberg, A.; Sjoblom, J.; Paso, K. Nanoparticles for waxy crudes: effect of polymer coverage and the effect on wax crystallization. *Energy Fuels* **2016**, *30*, 5108–5114.
- (63) Vijayakumar, S. D.; Ridzuan, N. Molecular interaction study on Gemini surfactant and nanoparticles in wax inhibition of Malaysian crude oil. *Asia-Pac. J. Chem. Eng.* **2021**, *16*, No. e2700.
- (64) Padula, L.; Gon, S.; Russell, C.; Pohl, E.; Littlehales, I.; Neilson, A. Systematic Study of Temperature and Different Types of Mixing in Paraffin Deposition Test Methods. *ACS Omega* **2020**, *5*, 12320–12328.
- (65) Bello, O.; Fasesan, S.; Teodoru, C.; Reinicke, K. An evaluation of the performance of selected wax inhibitors on paraffin deposition of Nigerian crude oils. *Pet. Sci. Technol.* **2006**, *24*, 195–206.
- (66) Silverstein, R. M.; Webster, F. X.; Kiemle, D. J.; Bryce, D. L. *Spectrometric Identification of Organic Compounds*; John Wiley & Sons, 2014.
- (67) Hanson, J. *Introduction to Interpretation of Infrared Spectra*, 2009.
- (68) Theyab, M.; Yahya, S. Introduction to wax deposition. *Int. J. Petrochem. Res.* **2018**, *2*, 126–131.
- (69) Bello, O.; Fasesan, S.; Macaulay, S.; Latinwo, G. *Study of the Influence of Xylene-Based Chemical Additive on Crude Oil Flow Properties and Paraffin Deposition Inhibition*; Qatar University, 2005.
- (70) Rodríguez, J.; Fuentes, E. M.; Espiridiao, M. C. A. Propiedades Interfaciales Del Surfactante Pdms-Peganhidrido Maléico-Ácido Fumárico (Pdms-Peg-Am-Af) En Solución Acuosa. *Rev. Colomb. Quím.* **2012**, *41*, 61–74.
- (71) Fernandez, A.; Salager, J.-L.; Scorzza, C. *Surfactantes*; Laboratorio FIRP: Mérida, Venezuela, 2004; pp 15–18.
- (72) Cabrera, F.; Cabrera, J.; Jimmy, D. Análisis y propuesta de mejora de proyectos de inyección de agua ejecutados en reservorios de diversas características. Tesis para optar por el Título de Ingeniero de Petróleos, Facultad de Ingeniería en Ciencias de la Tierra, Escuela Superior Politécnica del Litoral, Guayaquil, Ecuador. WEBGRAFÍA, 2012.
- (73) El-Dalatony, M. M.; Jeon, B.-H.; Salama, E.-S.; Eraky, M.; Kim, W. B.; Wang, J.; Ahn, T. Occurrence and characterization of paraffin wax formed in developing wells and pipelines. *Energies* **2019**, *12*, 967.
- (74) Said, M. S.; Jaafar, M. Z.; Omar, S.; Sharbini, S. N. Influence of whey protein isolate on CO₂ foams stability in three different types of crude oil. *Case Stud. Chem. Environ. Eng.* **2022**, *5*, 100191.
- (75) Mansourpoor, M.; Azin, R.; Osfouri, S.; Izadpanah, A. A. Experimental investigation of wax deposition from waxy oil mixtures. *Appl. Petrochem. Res.* **2019**, *9*, 77–90.
- (76) Fakoya, M. F.; Shah, S. N. Emergence of nanotechnology in the oil and gas industry: Emphasis on the application of silica nanoparticles. *Petroleum* **2017**, *3*, 391–405.
- (77) VijayaKumar, S.; Zakaria, J.; Ridzuan, N. The role of Gemini surfactant and SiO₂/SnO/Ni₂O₃ nanoparticles as flow improver of Malaysian crude oil. *J. King Saud Univ. Eng. Sci.* **2022**, *34*, 384–390.
- (78) Alsharaf, J. M.; Taha, M. R.; Khan, T. A. Physical Dispersion Of Nanocarbons In Composites A Review. *J. Teknol.* **2017**, *79*, 69.
- (79) Sun, M.; Rezaei, N.; Firoozabadi, A. Mitigating paraffin wax deposition by dispersants and crystal modifiers in flow testing. *Fuel* **2022**, *324*, 124687.
- (80) Hoffmann, R.; Amundsen, L. Influence of wax inhibitor on fluid and deposit properties. *J. Pet. Sci. Eng.* **2013**, *107*, 12–17.
- (81) Lashkarbolooki, M.; Seyfaee, A.; Esmailzadeh, F.; Mowla, D. Experimental investigation of wax deposition in Kermanshah crude oil through a monitored flow loop apparatus. *Energy Fuels* **2010**, *24*, 1234–1241.
- (82) Chi, Y.; Daraboina, N.; Sarica, C. Effect of the flow field on the wax deposition and performance of wax inhibitors: cold finger and flow loop testing. *Energy Fuels* **2017**, *31*, 4915–4924.